INSTABILITIES OF PERIODIC WAVES FOR THE LUGIATO-LEFEVER EQUATION

LUCIE DELCEY* & MARIANA HARAGUS†

Dedicated to Professor Philippe Ciarlet on the occasion of his eightieth birthday

Abstract

The Lugiato-Lefever equation arises as a model in nonlinear optics. Using tools from bifurcation theory, we study the existence and the stability of periodic steady waves which bifurcate from spatially constant solutions. For the stability problem, we focus on subharmonic perturbations, i.e., spatially periodic perturbations with periods equal to an integer multiple of the period of the steady wave.

AMS Subject Classification: 35Q60

Key Words: Lugiato-Lefever equation, periodic waves, bifurcations, instability

Running head: PERIODIC WAVES FOR THE LUGIATO-LEFEVER EQUATION

1 Introduction

The Lugiato-Lefever equation

$$\frac{\partial \psi}{\partial t} = -i\beta \frac{\partial^2 \psi}{\partial x^2} - (1 + i\alpha)\psi + i\psi|\psi|^2 + F, \tag{1.1}$$

is a nonlinear Schrödinger type equation with damping, detuning and driving, which has been derived in nonlinear optics by Lugiato and Lefever [7]. More recently, it has been used as a model for frequency combs, i.e., optical signals consisting of a superposition of modes with equally spaced frequencies, in whispering-gallery-mode resonators with Kerr nonlinearity [2]. In this context, the complex-valued unknown ψ, which depends upon the temporal variable t and the spatial variable x, represents the overall intracavity field, the real parameters α and β are the frequency detuning

*Laboratoire de mathématiques de Besançon, Univ. Bourgogne Franche-Comté, 16 route de Gray, 25030 Besançon cedex, France; lucie.delcey@univ-fcomte.fr.

†FEMTO-ST Institute, Univ. Bourgogne Franche-Comté, CNRS, 15B avenue des Montboucons, 25030 Besançon cedex, France; mariana.haragus@femto-st.fr.

and the overall dispersion parameters, respectively, and the positive constant F is the dimensionless external pump field intensity. Upon rescaling x, we may take $|\beta| = 1$, and we distinguish between normal dispersion, $\beta = 1$, and anomalous dispersion, $\beta = -1$.

The important questions for the physical problem concern the dynamics of nonlinear waves, and in particular the existence and the stability of steady periodic and localized waves. These questions have been intensively studied in the physics literature (e.g., see [1] and the references therein), but much less in the mathematics literature. The first rigorous mathematical results have been obtained in the case of anomalous dispersion in [9], where tools from local bifurcation theory have been used to study the existence of steady periodic and localized waves at the onset of Turing instability, where a stable constant solution becomes unstable with respect to periodic perturbations with nonzero wavenumbers. A systematic study of local bifurcations for steady bounded solutions, including steady periodic and localized solutions, have been done in [4, 5], whereas a study of global bifurcations of steady periodic solutions have been done in [8]. The stability problem is widely open, stability results have been obtained so far only for the steady periodic waves bifurcating at the onset of Turing instability, for co-periodic perturbations, i.e., periodic perturbations with period equal to the period of the steady wave, in [10], and for general bounded perturbations in [3].

The purpose of this paper is to study the existence and the stability of all steady periodic solutions bifurcating from constant solutions, without restricting to the onset of instability. The starting point of our analysis is the spectral stability analysis of constant solutions from [3], which allows us to precisely identify the parameter regions where steady periodic solutions bifurcate from constant solutions. It turns out that steady periodic solutions bifurcate at the onset of instability of constant solutions, on the one hand, and when these instabilities are fully developped, on the other hand. The solutions bifurcating at the onset of instability have been analyzed in [3]. Here, we discuss the solutions bifurcating when instabilities are fully developped.

In [3], two types of instabilities have been found for the constant solutions: the Turing instability mentioned above and a zero-mode instability, in which the instability of the constant solution is due to constant perturbations. For parameter values in the Turing instability region, we prove the existence of two families of steady periodic solutions with wavelengths $k_{\min} < k_{\max}$, whereas for parameter values in the zero-mode instability region we show the existence of one family of steady periodic solutions with wavelengths $k_{\max}$. The values $k_{\max}$ and $k_{\min}$ are precisely determined in terms of the physical parameters α, β, and F from the Lugiato-Lefever equation (1.1).

The existence proofs rely upon a formulation of the equation (1.1) as an infinite-dimensional dynamical system and a center manifold reduction. In this approach, the dynamics close to the bifurcation points is described by a two-dimensional reduced

system of ordinary differential equations, and the periodic steady solutions of the equation (1.1) are found as equilibria of this reduced system. We identify a steady bifurcation which, depending upon the values of the parameters, may be supercritical or subcritical. Besides the existence of periodic solutions, we can also conclude on their stability with respect to co-periodic perturbations: the periodic solutions are stable when the bifurcation is supercritical and unstable when the bifurcation is subcritical. For general bounded perturbations, all these solutions are unstable, due to the instability of the background constant solution which is fully developped, but they may be stable for particular classes of perturbations. Here, we focus on subharmonic perturbations, i.e., periodic perturbations with periods which are equal to an integer multiple of the period of the wave, which are of particular importance for the physical problem. We distinguish between background instabilities, which are due to instabilities of the background constant solution, and shape instabilities, which are induced by the periodic wave itself.

In our presentation, we focus on the case of anomalous dispersion which is analyzed in detail in Sections 2-4, and only summarize the results found in the case of normal dispersion in Section 5. We recall the stability results for constant solutions in Section 2, analyze the bifurcation problem in Section 3, and discuss the stability of the bifurcating steady periodic solutions in Section 4.

2 Stability of constant solutions

In this section, we summarize the stability properties of the constant solutions of the Lugiato-Lefever equation (1.1) in the case of anomalous dispersion, $\beta = -1$ (see [3] for more details).

Constant solutions $\psi \in \mathbb{C}$ of the equation (1.1) satisfy the algebraic equation

$$(1 + i\alpha)\psi - i\psi|\psi|^2 = F,$$

and upon setting $\psi = \psi_r + i\psi_i$ and $\rho = |\psi|^2 = \psi_r^2 + \psi_i^2$, a direct calculation gives

$$\psi_r = \frac{\rho}{F}, \quad \psi_i = \frac{\rho(\rho - \alpha)}{F}, \quad \rho\left((\rho - \alpha)^2 + 1\right) = F^2. \tag{2.1}$$

The monotonicity properties of the cubic polynomial in the left hand side of the last equation above determine the number of constant solutions: for any $\alpha \leqslant \sqrt{3}$ and $F > 0$ there is precisely one constant solution, whereas for $\alpha > \sqrt{3}$, there exist $F_-(\alpha) < F_+(\alpha)$,

$$F_\pm^2(\alpha) = \rho_\pm(\alpha)\left((\rho_\pm(\alpha) - \alpha)^2 + 1\right), \quad \rho_\pm(\alpha) = \frac{1}{3}\left(2\alpha \mp \sqrt{\alpha^2 - 3}\right),$$

such that the equation possesses three constant solutions with $\rho = \rho_j$, $j = 1, 2, 3$,

$$\rho_1 < \rho_+(\alpha) < \rho_2 < \rho_-(\alpha) < \rho_3,$$

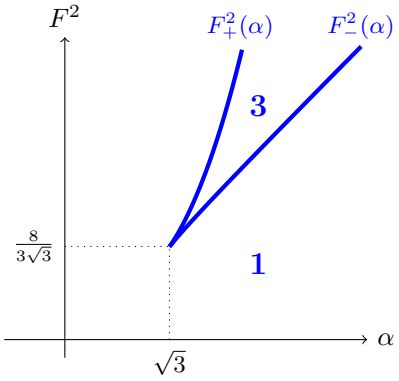

Figure 2.1: Number of constant solutions of the Lugiato-Lefever equation (1.1): three solutions in the region between the curves $F^2 = F_\pm^2(\alpha)$, two solutions along the curves, and one solution otherwise.

when $F_-(\alpha) < F < F_+(\alpha)$, two distinct constant solutions when $F = F_\pm(\alpha)$, and one constant solution when $F < F_-(\alpha)$ or $F_+(\alpha) < F$ (see Figure 2.1).

The linear stability of a constant solution $\psi^* = \psi_r^* + i\psi_i^*$ is determined by the spectrum of the 2×2 matrix operator $\mathcal{A}^*$ in the linear equation

$$\frac{dV}{dt} = \mathcal{A}^* V,$$

obtained by setting $\psi = \psi^* + (u + iv)$ in (1.1), $V = (u, v)^T$, and taking the real and imaginary parts of the resulting linearized equation. We find

$$\mathcal{A}^* = -\mathbb{I} + \mathcal{J}\mathcal{L}^*, \tag{2.2}$$

in which

$$\mathbb{I} = \begin{pmatrix} 1 & 0 \\ 0 & 1 \end{pmatrix}, \quad \mathcal{J} = \begin{pmatrix} 0 & -1 \\ 1 & 0 \end{pmatrix}, \tag{2.3}$$

and

$$\mathcal{L}^* = \begin{pmatrix} \partial_x^2 - \alpha + 3\psi_r^{*2} + \psi_i^{*2} & 2\psi_r^*\psi_i^* \\ 2\psi_r^*\psi_i^* & \partial_x^2 - \alpha + \psi_r^{*2} + 3\psi_i^{*2} \end{pmatrix}.$$

A standard Fourier analysis shows that the spectrum $\sigma(\mathcal{A}^*)$ of $\mathcal{A}^*$, in both the Hilbert space $L^2(\mathbb{R}) \times L^2(\mathbb{R})$ of square integrable functions and the Banach space $C_b(\mathbb{R}) \times C_b(\mathbb{R})$ of uniformly continuous functions, is given by

$$\sigma(\mathcal{A}^*) = \left\{ \lambda \in \mathbb{C} \,;\; \lambda^2 + 2\lambda + a(k) = 0,\; k \in \mathbb{R} \right\}, \tag{2.4}$$

in which

$$a(k) = k^4 + 2(\alpha - 2\rho^*)k^2 + \alpha^2 - 4\alpha\rho^* + 3\rho^{*2} + 1, \quad \rho^* = |\psi^*|^2 = \psi_r^{*2} + \psi_i^{*2}.$$

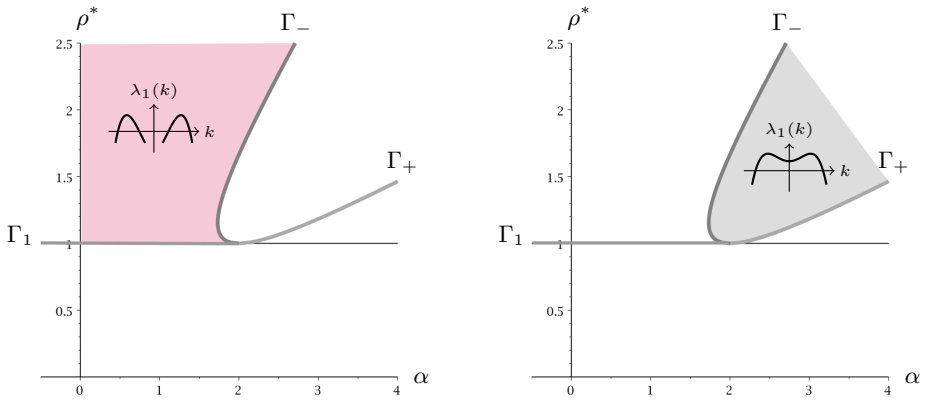

Figure 2.2: Stability of constant solutions in the case of anomalous dispersion. In the (α, ρ^*)-plane, the shaded regions represent the values for which a constant solution with $\rho^* = |\psi^*|^2$ is Turing unstable (left plot) and zero-mode unstable (right plot). The insets show a typical shape of the largest eigenvalue $\lambda_1(k)$ in these instability regions.

The constant solution ψ^* is unstable if one of the two roots $\lambda_{1,2}(k)$ of the quadratic polynomial in (2.4) has positive real part, for some wavelength $k \in \mathbb{R}$, and stable otherwise. Since the sum of these two roots is -2, we may take $\lambda_2(k) = -2 - \lambda_1(k)$ such that $\mathrm{Re}(\lambda_2(k)) \leqslant -1$ and $\mathrm{Re}(\lambda_1(k)) \geqslant -1$, for any $k \in \mathbb{R}$. Furthermore $\mathrm{Re}(\lambda_1(k)) > -1$ if and only if $\lambda_1(k)$ is real, and it is straightforward to check that $\lambda_1(k) > 0$ if and only if $a(k) < 0$. Consequently, instabilities are found when $\lambda_1(k) > 0$, or equivalently $a(k) < 0$, for some $k \in \mathbb{R}$.

According to the analysis in [3], two types of instabilities occur: a Turing instability when $\lambda_1(0) < 0$ and $\lambda_1(k) > 0$ for some $k \neq 0$, and a zero-mode instability when $\lambda_1(0) > 0$. The corresponding parameter values are found from the condition $a(k) < 0$ and are represented in Figure 2.2. The instability regions are determined by the values of α and ρ^*, only, the values of the parameter F and of the constant solution ψ^* being obtained from the equalities (2.1). The curves Γ_1, Γ_+, and Γ_-, which form the boundaries of these two regions, are defined through

$$\Gamma_1 = \{\alpha < 2,\ \rho^* = 1\}, \quad \Gamma_+ = \{\alpha > 2,\ \rho^* = \rho_+(\alpha)\}, \tag{2.5}$$

and

$$\Gamma_- = \{\sqrt{3} < \alpha < 2,\ \rho^* = \rho_+(\alpha)\} \cup \{\alpha > \sqrt{3},\ \rho^* = \rho_-(\alpha)\}. \tag{2.6}$$

A constant solution looses its stability upon increasing ρ^* and becomes Turing or zero-mode unstable when crossing the curves Γ_1 or Γ_+, respectively. The instability is fully developed in the open sets situated between the curves Γ_1 and Γ_- (Turing instability region) and the curves Γ_- and Γ_+ (zero-mode instability region).

Remark 2.1 *The three curves Γ_1, Γ_+, and Γ_- above are precisely the bifurcation curves found in the local bifurcation analysis of the steady Lugiato-Lefever equation in [5]. In the spatial dynamics approach from [5], the bifurcation points are the*

parameter values where the number of purely imaginary eigenvalues of a certain 4×4 *matrix changes. It turns out that these purely imaginary eigenvalues are precisely the values* ik *with* k *such that* $\lambda_1(k) = 0$*. This property implies that the curves* Γ_1*,* Γ_+*, and* Γ_- *correspond to the local bifurcations* $(i\omega)^2$*,* 0^2*, and* $0^2(i\omega)$*, respectively, studied [5].*

3 Bifurcation analysis

In this section, we study the bifurcations of steady periodic solutions which occur in the Turing and zero-mode instability regions defined in Section 2. We assume that the instabilities are fully developed, so that the boundaries Γ_1, Γ_+, and Γ_- are excluded from the analysis. We follow the approach used in [3] for the analysis of the onset of Turing instability, i.e., for parameter values $(\alpha, \rho^*) \in \Gamma_1$.

3.1 Dynamical system and choice of parameters

We fix (α, ρ^*) in either the Turing instability region, or the zero-mode instability region, denote by F_* the corresponding value of the parameter F given by (2.1), and take F as bifurcation parameter by setting $F^2 = F_*^2 + \mu$, with small μ.

For the Lugiato-Lefever equation (1.1), we look for spatially periodic solutions with wavelength $k_* > 0$ of the form

$$\psi(x,t) = \psi_\mu^* + (u+iv)(y,t), \quad y = k_* x, \tag{3.1}$$

where $\psi_\mu^* = \psi_{r\mu}^* + i\psi_{i\mu}^*$ is the constant solution given by (2.1) for $F^2 = F_*^2 + \mu$, and the functions u and v are real-valued and 2π-periodic in y. Inserting (3.1) into (1.1) we obtain a system of the form

$$\frac{dU}{dt} = \mathcal{A}_\mu^* U + \mathcal{F}(U,\mu), \tag{3.2}$$

for $U = (u,v)^T$, in which $\mathcal{A}_\mu^*$ is the linear operator

$$\mathcal{A}_\mu^* = -\mathbb{I} + \mathcal{J}\mathcal{L}_\mu^*,$$

with $\mathbb{I}$ and $\mathcal{J}$ the matrices defined by (2.3),

$$\mathcal{L}_\mu^* = \begin{pmatrix} k_*^2\partial_y^2 - \alpha + 3{\psi_{r\mu}^*}^2 + {\psi_{i\mu}^*}^2 & 2\psi_{r\mu}^*\psi_{i\mu}^* \\ 2\psi_{r\mu}^*\psi_{i\mu}^* & k_*^2\partial_y^2 - \alpha + {\psi_{r\mu}^*}^2 + 3{\psi_{i\mu}^*}^2 \end{pmatrix},$$

and $\mathcal{F}(U,\mu)$ is a nonlinear map,

$$\mathcal{F}(U,\mu) = \mathcal{J}\left(\mathcal{R}_2(U,U,\mu) + \mathcal{R}_3(U,U,U)\right),$$

where $\mathcal{R}_2(\cdot,\cdot,\mu)$ and $\mathcal{R}_3$ are bilinear and trilinear maps, respectively, such that

$$\mathcal{R}_2(U_1,U_2,\mu)=\begin{pmatrix}\psi^*_{r\mu}(3u_1u_2+v_1v_2)+\psi^*_{i\mu}(u_1v_2+u_2v_1)\\ \psi^*_{i\mu}(u_1u_2+3v_1v_2)+\psi^*_{r\mu}(u_1v_2+u_2v_1)\end{pmatrix}, \tag{3.3}$$

for $U_j=(u_j,v_j)^T$, $j=1,2$, and

$$\mathcal{R}_3(U,U,U)=\begin{pmatrix}u(u^2+v^2)\\ v(u^2+v^2)\end{pmatrix}, \tag{3.4}$$

for $U_j=(u,v)^T$.

We choose as phase-space for the dynamical system (3.2) the Hilbert space of 2π-periodic, square-integrable functions $\mathcal{X}=L^2(0,2\pi)\times L^2(0,2\pi)$. In this space, $\mathcal{A}^*_\mu$ is a closed linear operator with domain $\mathcal{Y}=H^2(0,2\pi)\times H^2(0,2\pi)$, $\mathcal{J}$ and $\mathcal{L}^*_\mu$ are skew- and self-adjoint operators, respectively, and $\mathcal{F}(\cdot,\mu):\mathcal{Y}\to\mathcal{Y}$ is a smooth map. Furthermore, as a consequence of the invariance of the Lugiato-Lefever equation (1.1) under the reflection $x\mapsto -x$ and under spatial translations $x\mapsto x+a$, $a\in\mathbb{R}$, the dynamical system (3.2) is equivariant under the actions of the reflection operator $\mathcal{T}$ and the translation operators $\mathcal{T}_a$ defined through

$$(\mathcal{T}U)(y)=U(-y),\quad (\mathcal{T}_aU)(y)=U(y+a),\quad y\in\mathbb{R}, \tag{3.5}$$

i.e., both $\mathcal{A}^*_\mu$ and $\mathcal{F}(\cdot,\mu)$ commute with $\mathcal{T}$ and $\mathcal{T}_a$, for any μ.

In this setting, we look for wavelengths k_* such that $\mu=0$ is a bifurcation point for the dynamical system (3.2). These bifurcation points are determined by the spectrum of the linear operator $\mathcal{A}^*_\mu$ at $\mu=0$. Since the domain $\mathcal{Y}$ of $\mathcal{A}^*_\mu$ is compactly embedded in $\mathcal{X}$, the operator has compact resolvent and therefore purely point spectrum consisting of isolated eigenvalues. Consequently, $\mu=0$ is a bifurcation point if the operator $\mathcal{A}^*_0$ possesses purely imaginary eigenvalues. Upon comparing $\mathcal{A}^*_0$ with the operator $\mathcal{A}^*$ given by (2.2) in Section 2, and taking into account the fact that the phase-space $\mathcal{X}$ consists of 2π-periodic functions, we find that the eigenvalues of $\mathcal{A}^*_0$ can be computed from the formula (2.4) by taking $k=nk_*$, $n\in\mathbb{Z}$, so that

$$\sigma(\mathcal{A}^*_0)=\{\lambda_1(nk_*),\ \lambda_2(nk_*),\ n\in\mathbb{Z}\},$$

where $\lambda_1(nk_*)$ and $\lambda_2(nk_*)$ are the two roots of the quadratic polynomial

$$\lambda^2+2\lambda+a(nk_*)=0.$$

With the notations from Section 2, $\mathrm{Re}(\lambda_1(k))>-1$ if and only if $\lambda_1(k)$ is real, so that $\mu=0$ is a bifurcation point when $\lambda_1(nk_*)=0$, for some $n\in\mathbb{Z}$. Without loss of generality we may assume $n=1$, otherwise we may replace k_* by nk_*. Taking into account the shape of $\lambda_1(k)$ (see the insets in Figure 2.2), for (α,ρ^*) in the Turing instability region there are precisely two positive values $k_{\min}<k_{\max}$ such

that $\lambda_1(k_{\min}) = \lambda_1(k_{\max}) = 0$, whereas in the zero-mode instability region there is only one positive value $k_{\max}$ such that $\lambda_1(k_{\max}) = 0$. We can compute these values from the condition $a(k) = 0$, which is equivalent to $\lambda_1(k) = 0$, and find

$$k_{\max}^2 = 2\rho^* - \alpha + \sqrt{\rho^{*2} - 1} \tag{3.6}$$

and

$$k_{\min}^2 = 2\rho^* - \alpha - \sqrt{\rho^{*2} - 1}. \tag{3.7}$$

Notice that $k_{\max}^2$ vanishes precisely along the curve Γ_+, whereas $k_{\min}^2$ vanishes along the curve Γ_-. In the next two subsections we study separately the bifurcations obtained for wavelengths $k_* = k_{\max}$ and $k_* = k_{\min}$.

3.2 Periodic solutions with wavelengths $k_{\max}$

For (α, ρ^*) fixed in either the Turing instability region, or the zero-mode instability region, we take $k_* = k_{\max}$. Then $\lambda_1(k_{\max}) = 0$, so that 0 is an eigenvalue of $\mathcal{A}_0^*$, and the results in Section 2 imply that all other eigenvalues in the spectrum $\sigma(\mathcal{A}_0^*)$ are either negative, or have negative real part equal to -1, in the Turing instability region, and that there exist an additional positive eigenvalue, with Fourier mode $n = 0$, in the zero-mode instability region. Consequently, we have the spectral decomposition

$$\sigma(\mathcal{A}_0^*) = \sigma_s(\mathcal{A}_0^*) \cup \sigma_c(\mathcal{A}_0^*) \cup \sigma_u(\mathcal{A}_0^*), \tag{3.8}$$

with

$$\sigma_c(\mathcal{A}_0^*) = \{0\}, \quad \sigma_s(\mathcal{A}_0^*) \cup \sigma_u(\mathcal{A}_0^*) \subset \{\lambda \in \mathbb{C} \,;\, |\operatorname{Re}\lambda| > \delta\},$$

for some $\delta > 0$, and $\sigma_u(\mathcal{A}_0^*) = \emptyset$ in the Turing instability region. A direct computation shows that 0 is a double semi-simple eigenvalue with associated eigenvectors ζ and $\overline{\zeta}$,

$$\zeta = \begin{pmatrix} (\rho^* - \sqrt{\rho^{*2} - 1})(\alpha + \sqrt{\rho^{*2} - 1}) \\ 2\rho^* - \alpha - \sqrt{\rho^{*2} - 1} \end{pmatrix} e^{iy}. \tag{3.9}$$

Following the approach in [3], we rewrite the system (3.2) in the form

$$\frac{dU}{dt} = \mathcal{A}_0^* U + \mathcal{G}(U, \mu), \tag{3.10}$$

in which

$$\mathcal{G}(U, \mu) = \mathcal{J}\left(\mathcal{R}_1(U, \mu) + \mathcal{R}_2(U, U, \mu) + \mathcal{R}_3(U, U, U)\right),$$

where $\mathcal{R}_1(\cdot, \mu) = \mathcal{L}_\mu^* - \mathcal{L}_0^*$ and $J, \mathcal{R}_2, \mathcal{R}_3$ are defined as before. Upon checking the hypotheses of the center manifold theorem [6, Chapter 2, Theorem 3.3], we conclude that the dynamical system (3.10) possesses a two-dimensional center manifold,

$$\mathcal{M}_c(\mu) = \{U \in \mathcal{Y} \,;\, U = A\zeta + \overline{A\zeta} + \Psi(A, \overline{A}, \mu),\ A \in \mathbb{C}\},$$

which contains all sufficiently small bounded solutions of (3.10), for any μ sufficiently small. Here Ψ is a map of class C^k, for any arbitrary but fixed $k \geqslant 3$, defined in a neighborhood of 0 in $\mathbb{C} \times \overline{\mathbb{C}} \times \mathbb{R}$, where $\mathbb{C} \times \overline{\mathbb{C}} = \{(A, \overline{A}) \ ; \ A \in \mathbb{C}\}$, and taking values in the spectral subspace $\mathcal{X}_h$ associated to the union $\sigma_s(\mathcal{A}_0^*) \cup \sigma_u(\mathcal{A}_0^*)$ of the stable and unstable spectra of the operator $\mathcal{A}_0^*$.

The dynamics on the center manifold $\mathcal{M}_c(\mu)$ is described by the reduced equation

$$\frac{dA}{dt} = f(A, \overline{A}, \mu), \tag{3.11}$$

in which f is a complex-valued map obtained by inserting the Ansatz

$$U = A\zeta + \overline{A\zeta} + \Psi(A, \overline{A}, \mu),$$

into the dynamical system (3.10) and then projecting on the eigenvector ζ. The symmetries (3.5) of the dynamical system (3.2) are inherited by the reduced system (3.11) which is $O(2)$-equivariant (see [3] for more details). As a consequence, the vector field f in (3.11) is of the form

$$f(A, \overline{A}, \mu) = Ag(|A|^2, \mu),$$

where g is a real-valued map of class C^{k-1} defined in a neighborhood of 0 in $\mathbb{R}^2$, and has the Taylor expansion

$$f(A, \overline{A}, \mu) = c_{11}\mu A + c_{30}A|A|^2 + \mathcal{O}(|A|(|\mu|^2 + |A|^4)). \tag{3.12}$$

The signs of the two real coefficients c_{11} and c_{30} determine the dynamics on the center manifold.

Assuming that both coefficients c_{11} and c_{30} are nonzero, the reduced system (3.11) undergoes a steady bifurcation with $O(2)$ symmetry at $\mu = 0$, which is supercritical when $c_{30} < 0$ and subcritical when $c_{30} > 0$. More precisely, we have the following properties (see also [6, Section 1.2.4]):

(i) If $c_{30}c_{11}\mu > 0$, then the reduced equation possesses a unique equilibrium $A = 0$ which is stable when $c_{30} < 0$, and unstable when $c_{30} > 0$.

(ii) If $c_{30}c_{11}\mu < 0$, then the reduced equation possesses the equilibrium $A = 0$ which is unstable when $c_{30} < 0$, and stable when $c_{30} > 0$, and a circle of nontrivial equilibria with opposite stability, $A_\mu(\phi) = r_\mu e^{i\phi}$, for $\phi \in \mathbb{R}/2\pi\mathbb{Z}$.

In contrast to [3], the computation of these coefficients is much more involved here. We summarize these computations in Appendix A. From the formulas (A.2) and (A.4) we conclude that both coefficients change sign when crossing the boundary Γ_- between the two instability regions, where $k_{\min}^2$ vanishes, and in addition c_{30} changes sign when crossing the curve Γ_{30} with cartesian equation $\widetilde{c}_{30} = 0$, where $\widetilde{c}_{30}$ is given

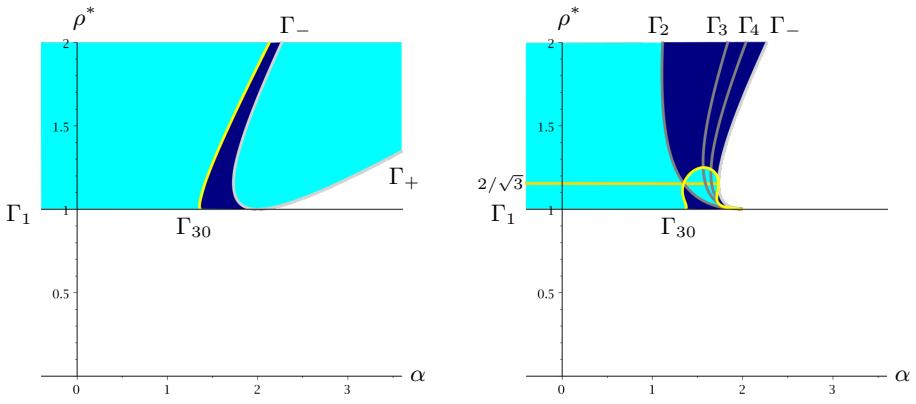

(a) $k_* = k_{\min}$ **(b)** $k_* = k_{\min}$

Figure 3.1: Bifurcations of steady periodic solutions in the case of anomalous dispersion. In the (α, ρ^*)-plane, the bifurcation is supercritical ($c_{30} < 0$) in the lighter shaded regions (light blue online) and subcritical ($c_{30} > 0$) in the darker shaded regions (navy blue online). In the case $k_* = k_{\min}$, we also represent the curves Γ_n, for $n = 2, 3, 4$, along which resonances occur, and the line $\rho^* = 2/\sqrt{3}$ along which c_{11} changes sign.

by (A.5). The curve Γ_{30} lies inside the Turing instability region, starting at the point $(\alpha, \rho^*) = (41/30, 1)$ and being asymptotic to Γ_-, as $\alpha \to \infty$ (see Figure 3.1a). Taking into account the signs of the coefficients c_{11} and c_{30} in the different parameter regions, from the properties (i) and (ii) above we obtain the following result.

Theorem 1 *Consider the Lugiato-Lefever equation (1.1) in the case $\beta = -1$ of anomalous dispersion. Assume that ψ^* is a constant solution of (1.1) with square modulus ρ^*, for parameter values α and F_*. If (α, ρ^*) belongs to either the Turing instability region, or the zero-mode instability region, as defined in Section 2, and does not belong to the curve Γ_{30}, then for $F^2 = F_*^2 + \mu$ and $k_* = k_{\max}$ the dynamical system (3.2) undergoes a steady bifurcation with $O(2)$ symmetry at $\mu = 0$, and the following properties hold.*

(i) If (α, ρ^*) belongs to the open set situated to the left of the curve Γ_{30} in the Turing instability region, then the coefficients of the reduced equation (3.11) satisfy $c_{11} > 0$ and $c_{30} < 0$, so that the bifurcation is supercritical and the reduced equation possesses a circle of stable nontrivial equilibria, $A_\mu(\phi) = r_\mu e^{i\phi}$, $\phi \in \mathbb{R}/2\pi\mathbb{Z}$, for any sufficiently small $\mu > 0$.

(ii) If (α, ρ^*) belongs to the open set situated to the right of the curve Γ_{30} in the Turing instability region, then the coefficients of the reduced equation (3.11) satisfy $c_{11} > 0$ and $c_{30} > 0$, so that the bifurcation is subcritical and the reduced equation possesses a circle of unstable nontrivial equilibria, $A_\mu(\phi) = r_\mu e^{i\phi}$, $\phi \in \mathbb{R}/2\pi\mathbb{Z}$, for any sufficiently small $\mu < 0$.

(iii) If (α, ρ^*) belongs to the zero-mode instability region, then the coefficients of the reduced equation (3.11) satisfy $c_{11} < 0$ and $c_{30} < 0$, so that the bifurcation

is supercritical and the reduced equation possesses a circle of stable nontrivial equilibria, $A_\mu(\phi) = r_\mu e^{i\phi}$, $\phi \in \mathbb{R}/2\pi\mathbb{Z}$, for any sufficiently small $\mu < 0$.

Going back to the Lugiato-Lefever equation (1.1), the circle of nontrivial equilibria $A_\mu(\phi) = r_\mu e^{i\phi}$ corresponds to a family of steady periodic solutions in x with wavelengths $k_{\max}$. The positive equilibrium $A_\mu(0) = r_\mu$ gives an even periodic solution of the Lugiato-Lefever equation (1.1), with Taylor expansion

$$\psi_\mu(x) = \psi^* + \psi_1 \cos(k_{\max}\, x)\, |\mu|^{1/2} + \mathcal{O}(|\mu|), \tag{3.13}$$

in which

$$\psi_1 = \left((\rho^* - \sqrt{\rho^{*2}-1})(\alpha + \sqrt{\rho^{*2}-1}) + i(2\rho^* - \alpha - \sqrt{\rho^{*2}-1})\right) \left|\frac{c_{11}}{c_{30}}\right|^{1/2},$$

whereas the other equilibria on the circle correspond to translations in x of this even periodic solution. This latter property is a consequence of the translation invariance of the Lugiato-Lefever equation (1.1).

3.3 Periodic solutions with wavelengths $k_{\min}$

We consider now (α, ρ^*) in the Turing instability region and take $k_* = k_{\min}$. Then 0 is an eigenvalue of $\mathcal{A}_0^*$, but in contrast to the case $k_* = k_{\max}$ above, its algebraic multiplicity is not always two. In this case, resonances occur for parameter values for which the two values $k_{\min} < k_{\max}$ are such that $k_{\max} = nk_{\min}$, for some $n \in \mathbb{N}$, $n \geqslant 2$. Then $\lambda_1(nk_{\min}) = 0$ and 0 is a quadruple eigenvalue of $\mathcal{A}_0^*$, with two additional eigenvectors in the Fourier mode n. We exclude these resonances from our analysis, since they lead to a four-dimensional, instead of a two-dimensional, reduced system which requires a different bifurcation analysis.

A direct calculation shows that a resonance $k_{\max} = nk_{\min}$, $n \geqslant 2$, occurs when

$$\alpha = 2\rho^* - \frac{n^2+1}{n^2-1}\sqrt{\rho^{*2}-1}. \tag{3.14}$$

This equality is the cartesian equation of a curve Γ_n in the (α, ρ^*)-plane, which starts at $(\alpha, \rho^*) = (2, 1)$ and lies in the Turing instability region. The curves Γ_2, Γ_3, and Γ_4 are represented in Figure 3.1b. As n increases, the curves Γ_n move to the right in the (α, ρ^*)-plane and accumulate at Γ_-, as $n \to \infty$. Assuming that (α, ρ^*) does not belong to any of the curves Γ_n, $n \geqslant 2$, the eigenvalue 0 of $\mathcal{A}_0^*$ is double and semi-simple with associated eigenvectors ζ and $\overline{\zeta}$ given by

$$\zeta = \begin{pmatrix} (\rho^* + \sqrt{\rho^{*2}-1})(\alpha - \sqrt{\rho^{*2}-1}) \\ 2\rho^* - \alpha + \sqrt{\rho^{*2}-1} \end{pmatrix} e^{iy}. \tag{3.15}$$

Furthermore, the spectral decomposition (3.8) holds, and $\sigma_u(\mathcal{A}_0^*)$ is empty for (α, ρ^*) in the open set situated to the left of the curve Γ_2, and above Γ_1, and contains precisely $n-1$ positive eigenvalues, $\lambda_1(jk_{\min})$, $j = 2, \dots, n$, for (α, ρ^*) in the open set between two consecutive curves Γ_n and Γ_{n+1}, $n \geqslant 2$.

Following the arguments used in the case $k_* = k_{\max}$, we obtain a reduced system of the same form (3.11), in which the coefficients c_{11} and c_{30} in the Taylor expansion (3.12) of f are given by the equalities (A.3) and (A.6), respectively, in Appendix A. In this case, the coefficient c_{11} vanishes when $\rho^* = 2/\sqrt{3}$, the coefficient c_{30} is not defined along the curve Γ_2 and vanishes along the curve Γ_{30} with cartesian equation $\widetilde{c}_{30} = 0$, where $\widetilde{c}_{30}$ is given by (A.7), and both coefficients change sign when crossing one of the curves where they vanish or are not defined. It is now straightforward to obtain the following result, similar to the one in Theorem 1.

Theorem 2 *Consider the Lugiato-Lefever equation (1.1) in the case $\beta = -1$ of anomalous dispersion. Assume that ψ^* is a constant solution of (1.1) with square modulus ρ^*, for parameter values α and F_*. If (α, ρ^*) belongs to the Turing instability region and does not belong to any of the curves Γ_n, $n \geqslant 2$, Γ_{30}, and $\rho^* = 2/\sqrt{3}$, then for $F^2 = F_*^2 + \mu$ and $k_* = k_{\min}$ the dynamical system (3.2) undergoes a steady bifurcation with $O(2)$ symmetry at $\mu = 0$, and the following properties hold.*

(i) If (α, ρ^*) belongs to the lighter shaded regions in Figure 3.1b and $\rho^* < 2/\sqrt{3}$, then $c_{11} > 0$ and $c_{30} < 0$, so that the bifurcation is supercritical and the reduced equation possesses a circle of stable nontrivial equilibria, $A_\mu(\phi) = r_\mu e^{i\phi}$, $\phi \in \mathbb{R}/2\pi\mathbb{Z}$, for any sufficiently small $\mu > 0$.

(ii) If (α, ρ^*) belongs to the lighter shaded regions in Figure 3.1b and $\rho^* > 2/\sqrt{3}$, then $c_{11} < 0$ and $c_{30} < 0$, so that the bifurcation is supercritical and the reduced equation possesses a circle of stable nontrivial equilibria, $A_\mu(\phi) = r_\mu e^{i\phi}$, $\phi \in \mathbb{R}/2\pi\mathbb{Z}$, for any sufficiently small $\mu < 0$.

(iii) If (α, ρ^*) belongs to the darker shaded regions in Figure 3.1b and $\rho^* < 2/\sqrt{3}$, then $c_{11} > 0$ and $c_{30} > 0$, so that the bifurcation is subcritical and the reduced equation possesses a circle of unstable nontrivial equilibria, $A_\mu(\phi) = r_\mu e^{i\phi}$, $\phi \in \mathbb{R}/2\pi\mathbb{Z}$, for any sufficiently small $\mu < 0$.

(iv) If (α, ρ^*) belongs to the darker shaded regions in Figure 3.1b and $\rho^* > 2/\sqrt{3}$, then $c_{11} < 0$ and $c_{30} > 0$, so that the bifurcation is subcritical and the reduced equation possesses a circle of unstable nontrivial equilibria, $A_\mu(\phi) = r_\mu e^{i\phi}$, $\phi \in \mathbb{R}/2\pi\mathbb{Z}$, for any sufficiently small $\mu > 0$.

Going back to the Lugiato-Lefever equation (1.1), the positive equilibrium $A_\mu(0) = r_\mu$ gives an even periodic solution of the Lugiato-Lefever equation (1.1), with Taylor expansion

$$\psi_\mu(x) = \psi^* + \psi_1 \cos(k_{\min}\, x)\, |\mu|^{1/2} + \mathcal{O}(|\mu|), \tag{3.16}$$

in which

$$\psi_1 = \Big((\rho^* + \sqrt{\rho^{*2}-1})(\alpha - \sqrt{\rho^{*2}-1}) + i(2\rho^* - \alpha + \sqrt{\rho^{*2}-1}) \Big) \left| \frac{c_{11}}{c_{30}} \right|^{1/2},$$

whereas the other equilibria on the circle correspond to translations in x of this even periodic solution.

4 Instabilities of periodic waves

In this section, we study the stability of the steady periodic solutions found in Section 3 in the two cases, $k_* = k_{\max}$ and $k_* = k_{\min}$. We focus on co-periodic and subharmonic perturbations, i.e., periodic perturbations with periods $2\pi N/k_*$, where $N = 1$ for co-periodic perturbations and $N \geqslant 2$ for subharmonic perturbations.

4.1 Background and shape instabilities

The bifurcation results in Section 3 also allow to conclude on the nonlinear stability of the bifurcating steady periodic solutions for perturbations which belong to the phase space $\mathcal{X} = L^2(0, 2\pi) \times L^2(0, 2\pi)$ of the dynamical system (3.2), i.e., for co-periodic perturbations which have the same period as the stationary solution. In this approach, the stability of a bifurcating solution $\psi_\mu(x)$ is determined by the location in the complex plane of the spectrum $\sigma(\mathcal{A}_0^*)$ of the operator $\mathcal{A}_0^*$, on the one hand, and by the stability of the corresponding equilibrium $A_\mu(\phi)$ of the reduced equation (3.11), on the other hand. More precisely, a bifurcating periodic solution $\psi_\mu(x)$ is stable if the spectrum $\sigma(\mathcal{A}_0^*)$ is stable, i.e., it does not contain eigenvalues with positive real part, and if the corresponding equilibrium $A_\mu(\phi)$ of the reduced equation is stable, as well. Then for initial data $\psi(x, 0) = \psi_\mu(x) + \phi_0(x)$, sufficiently close to a periodic wave $\psi_\mu(x)$, the solution $\psi(x, t)$ of the Lugiato-Lefever equation converges to a translated periodic wave $\psi_\mu(x + a)$, for some $a \in \mathbb{R}$,

$$\|\psi(\cdot, t) - \psi_\mu(\cdot + a)\|_{H^2_{\rm per}} \to 0, \qquad \text{as } t \to \infty. \tag{4.1}$$

The decay rate is given by the convergence rate towards equilibria on the center manifold, hence it is slowly exponential, $\mathcal{O}(e^{-d\mu})$, for some $d > 0$. If one of the two properties above does not hold then the bifurcating periodic solution $\psi_\mu(x)$ is unstable. We distinguish between two types of instabilities: background instabilities, when $\sigma(\mathcal{A}_0^*)$ contains eigenvalues with positive real part, and shape instabilities, when the equilibrium $A_\mu(\phi)$ of the reduced equation is unstable.

Upon replacing the phase space $\mathcal{X} = L^2(0, 2\pi) \times L^2(0, 2\pi)$ of 2π-periodic functions by the phase space $\mathcal{X}_N = L^2(0, 2\pi N) \times L^2(0, 2\pi N)$ of $2\pi N$-periodic functions, for some arbitrary, but fixed N, we can extend the class of perturbations from

co-periodic to subharmonic perturbations. The key difference is that now the spectrum of the operator $\mathcal{A}_0^*$ possesses additional eigenvalues,

$$\sigma(\mathcal{A}_0^*) = \{\lambda_1(nk_*/N),\ \lambda_2(nk_*/N),\ n \in \mathbb{Z}\}\,, \tag{4.2}$$

where $\lambda_1(nk_*/N)$ and $\lambda_2(nk_*/N)$ are the two roots of the quadratic polynomial

$$\lambda^2 + 2\lambda + a(nk_*/N) = 0.$$

As a consequence, the operator $\mathcal{A}_0^*$ may have additional unstable eigenvalues, hence leading to additional background instabilities, and more resonances may occur, as the ones found for $k_* = k_{\min}$ in Section 3, where the eigenvalue 0 is quadruple, instead of double. In the next two subsections we study separately the cases $k_* = k_{\max}$ and $k_* = k_{\min}$.

4.2 Periodic solutions with wavelengths $k_{\max}$

Consider the family of steady periodic solutions $\psi_\mu(x)$ with wavelengths $k_* = k_{\max}$ constructed in Theorem 1. For co-periodic perturbations, $N = 1$, their stability follows from the results in Section 3. The spectral decomposition (3.8) implies that the spectrum $\sigma(\mathcal{A}_0^*)$ is stable in the Turing instability region, whereas it contains one positive eigenvalue in the zero-mode instability region, and according to Theorem 1 the equilibria $A_\mu(\phi)$ are stable when the bifurcation is supercritical and unstable when the bifurcation is subcritical. Consequently, in the three cases in Theorem 1 the periodic solutions are stable in the case *(i)*, background stable and shape unstable in the case *(ii)*, and background unstable and shape stable in the case *(iii)*.

For subharmonic perturbations, $N \geqslant 2$, we consider the dynamical system (3.2) in the phase space $\mathcal{X}_N = L^2(0, 2\pi N) \times L^2(0, 2\pi N)$. In contrast to the case $N = 1$, for $N \geqslant 2$ resonances occur for certain parameter values, due to the presence of additional eigenvalues in the spectrum of $\mathcal{A}_0^*$. Indeed, the equality (4.2) implies that the eigenvalue 0 of the operator $\mathcal{A}_0^*$ is quadruple instead of double, hence a resonance occur, when $k_{\min} = nk_{\max}/N$, for $n = 1, \dots, N-1$. From the formulas (3.6) and (3.7) we obtain that $k_{\min} = nk_{\max}/N$ when the equalities

$$\alpha = 2\rho^* - \frac{N^2 + n^2}{N^2 - n^2}\sqrt{\rho^{*2} - 1} \tag{4.3}$$

hold, for $n = 1, \dots, N-1$. Each of these equalities defines a curve $\Gamma_{n,N}$ in the (α, ρ^*)-plane which lies in the Turing instability region. For increasing $n = 1, \dots, N-1$, these curves are ordered from right to the left between the curves Γ_- and Γ_1 in the (α, ρ^*)-plane. Notice that the values $n = 0$ and $n = N$ correspond to the curves Γ_- and Γ_1, respectively, and that $\Gamma_{1,N}$ is the curve Γ_N defined by (3.14) in Section 3.

Assuming that (α, ρ^*) does not belong to any of the curves $\Gamma_{n,N}$, $n = 1, \dots, N-1$, the spectral decomposition (3.8) holds, with 0 a double semi-simple eigenvalue. The unstable spectrum $\sigma_u(\mathcal{A}_0^*)$ is empty for (α, ρ^*) in the open set between the curves Γ_1 and $\Gamma_{N-1,N}$, it consists of $N-n$ positive eigenvalues in the open set between two consecutive curves $\Gamma_{n,N}$ and $\Gamma_{n-1,N}$, for any $n = 2, \dots, N-1$, of $N-1$ positive eigenvalues in the open set between $\Gamma_{1,N}$ and Γ_-, and of N positive eigenvalues for (α, ρ^*) in the zero-mode instability region. In particular, this shows that the periodic solution is background stable with respect to $2\pi N/k_{\max}$-periodic perturbations when (α, ρ^*) belongs to the open set between the curves Γ_1 and $\Gamma_{N-1,N}$, and it is background unstable otherwise.

Next, we find the shape instabilities by applying the center manifold reduction, as in Section 3. Since the eigenvalue 0 is double, the center manifold is two-dimensional, and it turns out that the reduced dynamics is governed by the same reduced system (3.11). Consequently, the result in Theorem 1 holds in $\mathcal{X}_N$, for any N, implying that shape instabilities occur only for the periodic solutions obtained in the subcritical bifurcation.

Along the resonance curves $\Gamma_{n,N}$, $n = 1, \dots, N-1$, the eigenvalue 0 of $\mathcal{A}_0^*$ is quadruple, and the center manifold reduction leads to a four-dimensional, instead of a two-dimensional system, just as in the case $k_* = k_{\min}$ in Section 3. The present bifurcation analysis does not allow to detect shape instabilities along these curves, but we can conclude that background instabilities occur along $\Gamma_{n,N}$, $n = 1, \dots, N-2$.

We summarize the main stability results above in the following theorem (see also Figure 4.1a).

Theorem 3 *Consider the Lugiato-Lefever equation (1.1) in the case $\beta = -1$ of anomalous dispersion, and the steady periodic solutions $\psi_\mu(x)$ given by (3.13), with wavelengths $k_{\max}$ and the properties in Theorem 1. For any $N \geqslant 2$, consider the curve $\Gamma_{N-1,N}$ defined through (4.3), and set $\Gamma_{0,1} = \Gamma_-$. Then the following stability properties hold for periodic perturbations with periods $2\pi N/k_{\max}$, for any $N \geqslant 1$.*

(i) If (α, ρ^*) belongs to the open set situated to the left of the curve $\Gamma_{N-1,N}$ in the Turing instability region, then the steady periodic solutions found in the supercritical bifurcation are stable, whereas the steady periodic solutions found in the subcritical bifurcation are unstable and the instability is a shape instability.

(ii) If (α, ρ^*) belongs to the open set situated to the right of the curve $\Gamma_{N-1,N}$ in the Turing instability region, then the steady periodic solutions are unstable; the instability is a background instability for the solutions found in the supercritical bifurcation, whereas the solutions found in the subcritical bifurcation are both background and shape unstable.

(iii) If (α, ρ^*) belongs to the zero-mode instability region, then the steady periodic solutions are unstable and the instability is a background instability.

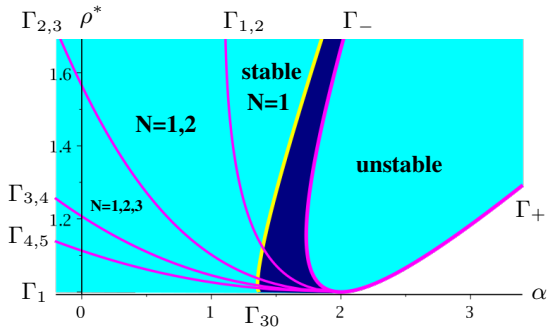

(a) $k_* = k_{\max}$

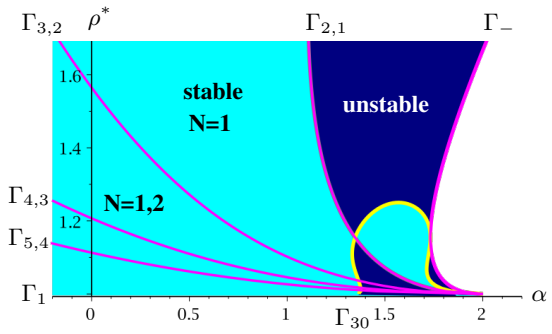

(b) $k_* = k_{\min}$

Figure 4.1: Stability of steady periodic solutions in the case of anomalous dispersion. In the (α, ρ^*)-plane, the steady periodic solutions are background stable for subharmonic perturbations with periods $2\pi N/k_*$ for the values of N as indicated, and unstable otherwise. In the lighter shaded regions (light blue online) they are shape stable, whereas in the darker shaded regions (navy blue online) they are shape unstable. The curves $\Gamma_{n,N}$ are defined by (4.3) in the case $k_* = k_{\max}$ and by (4.4) in the case $k_* = k_{\min}$.

4.3 Periodic solutions with wavelengths $k_{\min}$

The stability of the family of steady periodic solutions with wavelengths $k_* = k_{\min}$ found in Theorem 2 is studied in the same way. In this case resonances occur when $k_{\max} = nk_{\min}/N$, for $n \geqslant N+1$, and using the formulas (3.6) and (3.7) we obtain a sequence of curves $\Gamma_{n,N}$, $n \geqslant N+1$, in the (α, ρ^*)-plane with parametric equations

$$\alpha = 2\rho^* + \frac{N^2+n^2}{N^2-n^2}\sqrt{\rho^{*2}-1}. \tag{4.4}$$

Notice that the curves $\Gamma_{n,1}$, for $N = 1$, are the curves Γ_n defined by (3.14) in Section 3. Using the same arguments as in the case $k_* = k_{\max}$, we obtain the following stability result (see also Figure 4.1b).

Theorem 4 *Consider the Lugiato-Lefever equation (1.1) in the case $\beta = -1$ of anomalous dispersion, and the steady periodic solutions $\psi_\mu(x)$ given by (3.16), with wavelengths $k_{\min}$ and the properties in Theorem 2. For any $N \geqslant 1$, consider the*

curve $\Gamma_{N+1,N}$ defined through (4.4). Then the following stability properties hold for periodic perturbations with periods $2\pi N/k_{\min}$, for any $N \geqslant 1$.

(i) If (α, ρ^*) belongs to the open set situated to the left of the curve $\Gamma_{N+1,N}$ in the Turing instability region, then the steady periodic solutions found in the supercritical bifurcation are stable, whereas the steady periodic solutions found in the subcritical bifurcation are unstable and the instability is a shape instability.

(ii) If (α, ρ^*) belongs to the open set situated to the right of the curve $\Gamma_{N+1,N}$ in the Turing instability region, then the steady periodic solutions are unstable; the instability is a background instability for the solutions found in the supercritical bifurcation, whereas the solutions found in the subcritical bifurcation are both background and shape unstable.

5 The case of normal dispersion

In this section we briefly discuss the case $\beta = 1$ of normal dispersion. The main difference with the case $\beta = -1$ of anomalous dispersion occurs in the linear stability analysis of constant solutions. This implies that the periodic waves bifurcate in different parameter regions, but the bifurcation and stability analysis in Sections 3-4 remain the same, including computations.

5.1 Stability of constant solutions

The constant solutions of the Lugiato-Lefever equation (1.1) are the same in both cases of normal and of anomalous dispersion (see Figure 2.1), but they have different stability properties. For a constant solution $\psi^* = \psi_r^* + i\psi_i^*$, with modulus square ρ^*, the linear operator $\mathcal{A}^*$ has the same form (2.2), but the linear operator $\mathcal{L}^*$ changes in the case of normal dispersion, the terms ∂_x^2 having now a coefficient -1,

$$\mathcal{L}^* = \begin{pmatrix} -\partial_x^2 - \alpha + 3\psi_r^{*2} + \psi_i^{*2} & 2\psi_r^*\psi_i^* \\ 2\psi_r^*\psi_i^* & -\partial_x^2 - \alpha + \psi_r^{*2} + 3\psi_i^{*2} \end{pmatrix}.$$

As a consequence, the sign of the coefficient of k^2 changes in the formula of $a(k)$ in the spectrum of linear operator $\mathcal{A}^*$,

$$\sigma(\mathcal{A}^*) = \left\{ \lambda \in \mathbb{C} \ : \ \lambda^2 + 2\lambda + a(k) = 0, \ k \in \mathbb{R} \right\},$$

in which

$$a(k) = k^4 - 2(\alpha - 2\rho^*)k^2 + \alpha^2 - 4\alpha\rho^* + 3\rho^{*2} + 1.$$

This implies a change in the stability properties of the constant solutions (see [3]). The zero-mode instability region is the same, but the Turing instability region is now

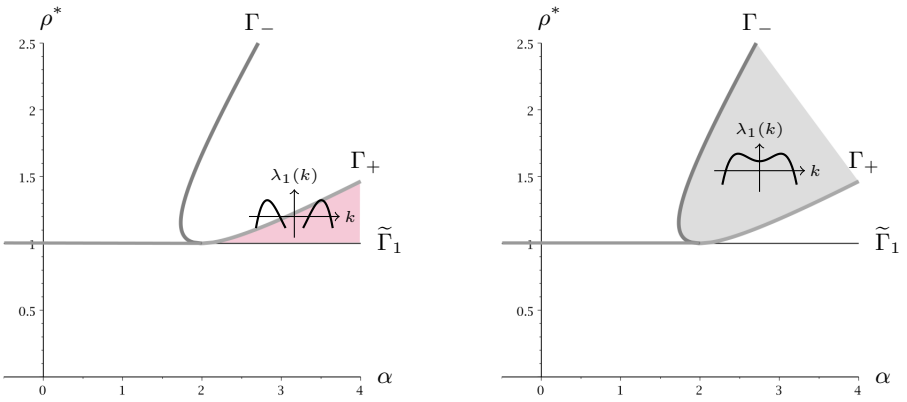

Figure 5.1: Stability of constant solutions in the case of normal dispersion. In the (α, ρ^*)-plane, the shaded regions represent the values for which a constant solution with $\rho^* = |\psi^*|^2$ is Turing unstable (left plot) and zero-mode unstable (right plot). The insets show a typical shape of the largest eigenvalue $\lambda_1(k)$ in these instability regions.

situated between the curve Γ_+ defined in (2.5) and the half-line

$$\widetilde{\Gamma}_1 = \{\alpha > 2,\ \rho^* = 1\}.$$

These regions are represented in Figure 5.1.

5.2 Bifurcations and stability of periodic solutions

As in the case of anomalous dispersion, in the Turing instability region we expect bifurcations of steady periodic solutions with wavelengths $k_* = \widetilde{k}_{\rm min}$ and $k_* = \widetilde{k}_{\rm max}$, where $\widetilde{k}_{\rm min} < \widetilde{k}_{\rm max}$ are such that $\lambda_1(\widetilde{k}_{\rm min}) = \lambda_1(\widetilde{k}_{\rm max}) = 0$, whereas in the zero-mode instability region we expect bifurcations of steady periodic solutions with wavelengths $k_* = \widetilde{k}_{\rm max}$. Since the difference between the formulas of $a(k)$ in the two cases is only a change of the sign of the coefficient of k^2, we find that

$$\widetilde{k}^2_{\rm max} = -k^2_{\rm min}, \quad \widetilde{k}^2_{\rm min} = -k^2_{\rm max},$$

where $k_{\rm max}$ and $k_{\rm min}$ are the wavelengths given by (3.6) and (3.7), respectively. Together with the fact that in the Lugiato-Lefever equation (1.1) the difference between the two cases of normal and anomalous dispersion is the sign of β, this implies that the dynamical systems found for $k_* = \widetilde{k}_{\rm max}$ and $k_* = \widetilde{k}_{\rm min}$ in the case of normal dispersion are precisely the ones found in the case of anomalous dispersion for $k_* = k_{\rm min}$ and $k_* = k_{\rm max}$, respectively. As a consequence, the calculations are the same as the ones in Sections 3 and 4, with the only difference that (α, ρ^*) belongs to a different parameter region in the case of the Turing instability. We do not give the precise statements of the analogue of Theorems 1–4 in this case, but only summarize the results in Figure 5.2.

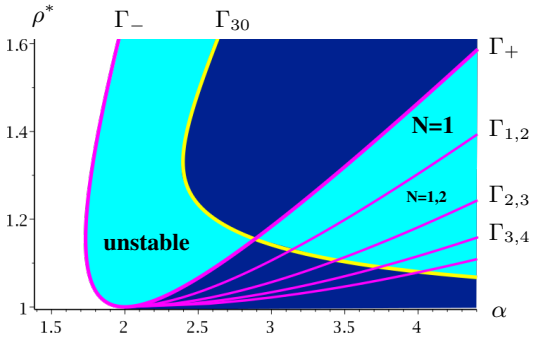

(a) $k_* = \widetilde{k}_{\max}$

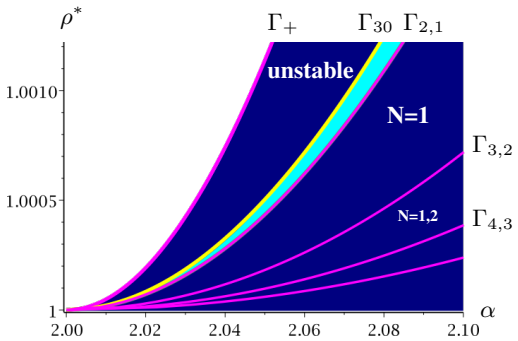

(b) $k_* = \widetilde{k}_{\min}$

Figure 5.2: Stability of steady periodic solutions in the case of normal dispersion. In the (α, ρ^*)-plane, the steady periodic solutions are background stable for subharmonic perturbations with periods $2\pi N/k_*$ for the values of N as indicated, and unstable otherwise. In the lighter shaded regions (light blue online) they are shape stable, whereas in the darker shaded regions (navy blue online) they are shape unstable. The curves $\Gamma_{n,N}$ are defined by (4.4) in the case $k_* = \widetilde{k}_{\max}$ and by (4.3) in the case $k_* = \widetilde{k}_{\min}$.

A Coefficients of the reduced system

A.1 Computation of c_{11}

According to [3], the coefficient c_{11} in the Taylor expansion (3.12) of the reduced vector field f can be computed from the formula

$$c_{11} = \frac{d\lambda_*}{d\mu}(0),$$

where $\lambda_*(\mu)$ is the eigenvalue of the operator $\mathcal{A}^*_\mu$ which is the continuation of the eigenvalue 0 of the operator $\mathcal{A}^*_0$, for small μ. The results in Section 2 imply that $\lambda_*(\mu)$ is the largest root of the polynomial

$$\lambda^2 + 2\lambda + a_\mu(k_*) = 0, \tag{A.1}$$

in which

$$a_\mu(k_*) = k_*^4 + 2(\alpha - 2\rho^*_\mu)k_*^2 + \alpha^2 - 4\alpha\rho^*_\mu + 3{\rho^*_\mu}^2 + 1,$$

and ρ_μ^* is the square modulus of the constant solution ψ_μ^* in (3.1), $\rho_\mu^* = |\psi_\mu^*|^2$. Upon differentiating (A.1) with respect to μ and taking $\mu = 0$, after some elementary calculations, we obtain

$$c_{11} = \frac{1}{k_{\max}^2 k_{\min}^2} \left(\rho^* + 2\sqrt{\rho^{*2} - 1}\right), \tag{A.2}$$

in the case $k_* = k_{\max}$, and

$$c_{11} = \frac{1}{k_{\max}^2 k_{\min}^2} \left(\rho^* - 2\sqrt{\rho^{*2} - 1}\right), \tag{A.3}$$

in the case $k_* = k_{\min}$. Notice that we can obtain the formula for $k_* = k_{\min}$ from the one for $k_* = k_{\max}$ just by changing the sign of the square root $\sqrt{\rho^{*2} - 1}$.

A.2 Computation of c_{30}

According to [3], the coefficient c_{30} in the Taylor expansion (3.12) can be computed from the formula

$$c_{30} = \frac{1}{\langle \zeta, \mathcal{J}\zeta_2 \rangle} \left\langle 2\mathcal{R}_2(\zeta, \Psi_{11}, 0) + 2\mathcal{R}_2(\overline{\zeta}, \Psi_{20}, 0) + 3\mathcal{R}_3(\zeta, \zeta, \overline{\zeta}), \zeta_2 \right\rangle,$$

in which $\mathcal{R}_2$ and $\mathcal{R}_3$ are the bilinear and trilinear maps, respectively, given by (3.3)-(3.4), ζ and ζ_2 are eigenvectors of $\mathcal{A}_0^*$ associated to the eigenvalues 0 and -2, respectively, and the vectors Ψ_{11} and Ψ_{20} are solutions of the linear equations:

$$\mathcal{A}_0^* \Psi_{11} = -2\mathcal{J}\mathcal{R}_2(\zeta, \overline{\zeta}, 0), \quad A_0^* \Psi_{20} = -\mathcal{J}\mathcal{R}_2(\zeta, \zeta, 0).$$

In the case $k_* = k_{\max}$, the eigenvector ζ is given by (3.9) and a direct calculation gives

$$\zeta_2 = \begin{pmatrix} (\rho^* - \sqrt{\rho^{*2} - 1})(2\rho^* - \alpha + \sqrt{\rho^{*2} - 1}) \\ -\alpha + \sqrt{\rho^{*2} - 1} \end{pmatrix} e^{iy}.$$

A symbolic computation using Maple gives

$$\Psi_{11} = \frac{4F_*}{k_{\max}^2\, k_{\min}^2} \begin{pmatrix} u_{11} \\ v_{11} \end{pmatrix},$$

$$\Psi_{20} = \frac{2F_*}{k_{\max}^2 (9(2\rho^* - \alpha) + 15\sqrt{\rho^{*2} - 1})} \begin{pmatrix} u_{20} \\ v_{20} \end{pmatrix} e^{2iy},$$

in which

$$\begin{aligned}
u_{11} &= (\rho^* - \sqrt{\rho^{*2}-1})\alpha^2 + (2\rho^*\sqrt{\rho^{*2}-1} - 2\rho^{*2} + 2)\alpha \\
&\quad -\rho^{*2}\sqrt{\rho^{*2}-1} + \rho^{*3} + \sqrt{\rho^{*2}-1} - 3\rho^*, \\
v_{11} &= (\rho^*\sqrt{\rho^{*2}-1} - \rho^{*2} - 1)\alpha^2 \\
&\quad -2(\rho^{*2}\sqrt{\rho^{*2}-1} - \rho^{*3} + \sqrt{\rho^{*2}-1} - 2\rho^*)\alpha \\
&\quad +\rho^{*3}\sqrt{\rho^{*2}-1} - \rho^{*4} + 3\rho^*\sqrt{\rho^{*2}-1} - 4\rho^{*2} + 1, \\
u_{20} &= 3(\sqrt{\rho^{*2}-1} - \rho^*)\alpha^2 - 2(\rho^*\sqrt{\rho^{*2}-1} - \rho^{*2} - 1)\alpha \\
&\quad -\rho^{*2}\sqrt{\rho^{*2}-1} + \rho^{*3} + 5\sqrt{\rho^{*2}-1} + 5\rho^*, \\
v_{20} &= -3(\rho^*\sqrt{\rho^{*2}-1} - \rho^{*2} - 1)\alpha^2 \\
&\quad +2(3\rho^{*2}\sqrt{\rho^{*2}-1} - 3\rho^{*3} - \sqrt{\rho^{*2}-1} - 8\rho^*)\alpha \\
&\quad -3\rho^{*3}\sqrt{\rho^{*2}-1} + 3\rho^{*4} + 3\rho^*\sqrt{\rho^{*2}-1} + 12\rho^{*2} + 5,
\end{aligned}$$

and then the formula for the coefficient c_{30},

$$c_{30} = \frac{2F_*^2(\rho^* - \sqrt{\rho^{*2}-1})}{k_{\max}^2 k_{\min}^2 (9(2\rho^* - \alpha) + 15\sqrt{\rho^{*2}-1})}\,\widetilde{c}_{30}, \tag{A.4}$$

where

$$\begin{aligned}
\widetilde{c}_{30} &= -27\sqrt{\rho^{*2}-1}\alpha^3 + 3(4\rho^*\sqrt{\rho^{*2}-1} - 25\rho^{*2} + 5)\alpha^2 \\
&\quad +(345\rho^{*2}\sqrt{\rho^{*2}-1} + 438\rho^{*3} - 67\sqrt{\rho^{*2}-1} - 236\rho^*)\alpha \\
&\quad -330\rho^{*3}\sqrt{\rho^{*2}-1} - 363\rho^{*4} + 144\rho^{*2} + 55.
\end{aligned} \tag{A.5}$$

Finally, as for the coefficient c_{11}, we obtain the formula for the coefficient c_{30} in the case $k_* = k_{\min}$ by changing the sign of the square root $\sqrt{\rho^{*2}-1}$ in the formula (A.4) for $k_* = k_{\max}$, so that

$$c_{30} = \frac{2F_*^2(\rho^* + \sqrt{\rho^{*2}-1})}{k_{\max}^2 k_{\min}^2 (9(2\rho^* - \alpha) - 15\sqrt{\rho^{*2}-1})}\,\widetilde{c}_{30}, \tag{A.6}$$

where

$$\begin{aligned}
\widetilde{c}_{30} &= 27\sqrt{\rho^{*2}-1}\alpha^3 - 3(4\rho^*\sqrt{\rho^{*2}-1} + 25\rho^{*2} - 5)\alpha^2 \\
&\quad -(345\rho^{*2}\sqrt{\rho^{*2}-1} - 438\rho^{*3} - 67\sqrt{\rho^{*2}-1} + 236\rho^*)\alpha \\
&\quad +330\rho^{*3}\sqrt{\rho^{*2}-1} - 363\rho^{*4} + 144\rho^{*2} + 55.
\end{aligned} \tag{A.7}$$

Acknowledgments: This work was partially supported by a doctoral grant of the Franche-Comté region (L.D.) and the Labex ACTION program, ANR-11-LABX-01-01 (M.H.).

References

[1] Y. K. Chembo, D. Gomila, M. Tlidi and C. R. Menyuk, *Topical Issue: Theory and Applications of the Lugiato-Lefever Equation.* Eur. Phys. J. D **71** (2017).

[2] Y. K. Chembo and C. R. Menyuk, *Spatiotemporal Lugiato-Lefever formalism for Kerr-comb generation in whispering-gallery-mode resonators.* Phys. Rev. A **87** (2013), 053852.

[3] L. Delcey and M. Haragus, *Periodic waves of the Lugiato-Lefever equation at the onset of Turing instability.* Phil. Trans. R. Soc. A **376** (2018), 20170188.

[4] C. Godey, I. Balakireva, A. Coillet and Y. K. Chembo, *Stability analysis of the spatiotemporal Lugiato-Lefever model for Kerr optical frequency combs in the anomalous and normal dispersion regimes.* Phys. Rev. A **89** (2014), 063814.

[5] C. Godey, *A bifurcation analysis for the Lugiato-Lefever equation.* Eur. Phys. J. D **71** (2017), 131.

[6] M. Haragus and G. Iooss, *Local bifurcations, center manifolds, and normal forms in infinite-dimensional dynamical systems.* Universitext. Springer-Verlag London, Ltd., London; EDP Sciences, Les Ulis, 2011.

[7] L. A. Lugiato and R. Lefever, *Spatial dissipative structures in passive optical systems.* Physical Review Letters **58** (1987), 2209.

[8] R. Mandel and W. Reichel, *A priori bounds and global bifurcation results for frequency combs modeled by the Lugiato-Lefever equation.* SIAM J. Appl. Math. **77** (2017), 315–345.

[9] T. Miyaji, I. Ohnishi and Y. Tsutsumi, *Bifurcation analysis to the Lugiato-Lefever equation in one space dimension.* Phys. D **239** (2010), 2066–2083.

[10] T. Miyaji, I. Ohnishi and Y. Tsutsumi, *Stability of a stationary solution for the Lugiato-Lefever equation.* Tohoku Math. J. (2) **63** (2011), 651–663.